UCRL-10316

University of California

Ernest O. Lawrence Radiation Laboratory

PLASTIC DEFORMATION OF MgO SINGLE CRYSTALS UNDER TO 1600° C

TWO-WEEK LOAN COPY

This is a Library Circulating Copy
which may be borrowed for two weeks.
For a personal retention copy, call
Tech. Info. Division, Ext. 5545

Berkeley, California

DISCLAIMER

This document was prepared as an account of work sponsored by the United States Government. While this document is believed to contain correct information, neither the United States Government nor any agency thereof, nor the Regents of the University of California, nor any of their employees, makes any warranty, express or implied, or assumes any legal responsibility for the accuracy, completeness, or usefulness of any information, apparatus, product, or process disclosed, or represents that its use would not infringe privately owned rights. Reference herein to any specific commercial product, process, or service by its trade name, trademark, manufacturer, or otherwise, does not necessarily constitute or imply its endorsement, recommendation, or favoring by the United States Government or any agency thereof, or the Regents of the University of California. The views and opinions of authors expressed herein do not necessarily state or reflect those of the United States Government or any agency thereof or the Regents of the University of California.

Submitted to J. Am. Ceramic Society

UCRL-10316

UNIVERSITY OF CALIFORNIA

Lawrence Radiation Laboratory
Berkeley, California

AEC Contract No. W-7405-eng-48

PLASTIC DEFORMATION OF MgO SINGLE CRYSTALS UP TO 1600°C

Stephen M. Copley and Joseph A. Pask

April 7, 1964

PLASTIC DEFORMATION OF MgO SINGLE CRYSTALS UP TO 1600° C

Stephen M. Copley and Joseph A. Pask

Department of Mineral Technology,
Inorganic Materials Research Division
of Lawrence Radiation Laboratory
University of California, Berkeley, California

April 7, 1964

ABSTRACT

Stress-strain curves are presented for MgO single crystals, compressed with ⟨100⟩ and ⟨111⟩ stress axes, for temperatures of 1000 to 1600° C. The yield stress of ⟨100⟩ specimens decreases slightly in this temperature range. The strain-hardening rate passes through a maximum at about 1100° C and decreases by a factor of about 8 at 1600° C. Above this temperature, the strain rate of ⟨100⟩ specimens is much less sensitive to changes in stress and the shape of the stress-strain curves changes. The yield stress of ⟨111⟩ specimens decreases rapidly with increasing temperature without a change of slope up to 1600° C. The ratio of the yield stresses for ⟨111⟩ and ⟨100⟩ specimens decreases continually from 1200 to 1600° C.

Part presented at the Fifteenth Pacific Coast Regional Meeting, The American Ceramic Society, Seattle, Washington, October 18, 1962 (Basic Science Division) and part at the Sixteenth Pacific Coast Regional Meeting, Los Angeles, California, October 25, 1963 (Properties of Ceramics Symposium).

This paper is based on part of a thesis submitted by Stephen M. Copley in partial fulfillment of the requirements for the degree of Doctor of Philosophy in engineering science, University of California, Berkeley, California, June 1964.

At the time this work was done the writers were, respectively, research assistant and professor of ceramic engineering, Department of Mineral Technology and Inorganic Materials Research Division, Lawrence Radiation Laboratory, University of California at Berkeley. S. M. Copley is now associated with the Advanced Materials Research and Development Laboratory, Pratt and Whitney Aircraft, North Haven, Connecticut.

Various stress rates were used to obtain a measure of strain hardening at 1300° C. Static recovery experiments were carried out at 1000 and 1400° C. At 1000° C static pinning occurred during the unloaded period; at 1400° C, "orthorecovery" occurred.

Stress-strain curves were analyzed by a dynamic approach based on the length of moving dislocation line in the crystal and the average dislocation velocity.

I. INTRODUCTION

Investigations of stress-strain behavior and the distribution of dislocations in deformed single-crystal specimens have led to a more detailed understanding of the mechanism of plastic deformation of MgO at room temperature. Stokes, Johnston, and Li have shown that dislocation movement is initiated on $\{110\}\ \langle 1\bar{1}0\rangle$ slip systems by the expansion of dislocation half loops which are present at cleavage steps, scratches, and other points of damage at the crystal surface.[1] Johnston and Gilman have measured the expansion velocities of individual dislocation half loops in LiF and have shown that they vary with temperature and impurity content and are extremely sensitive to stress.[2] Johnston has observed a similar behavior in the case of MgO.[3]

As a dislocation loop expands, it leaves in its wake "debris" in the form of elongated edge dislocation pairs or dipoles, which have been directly observed by Washburn and coworkers in thin foils of MgO with the electron microscope.[4,5] These dipoles obstruct further dislocation movement on active slip planes but also provide the mechanism for spreading of mobile dislocation lines to adjacent atomic planes.[5] Because dislocation movement within slip bands is obstructed by the presence of dipoles, most movement occurs at slip band edges through undeformed regions.[6] Hoover and Washburn have shown that subsequent to yielding the length of mobile dislocation in LiF is proportional to the number of interfaces between slip bands and undeformed material.[7] Strain hardening was not observed until slip band overlap and intersection became important.

At elevated temperatures, much less is known about the relationship of dislocation behavior to the plastic deformation of MgO. Hulse and Pask,[8] Thompson and Roberts,[9] and also May and Kronberg[10] have studied the stress-strain behavior of MgO single crystals compressed in a ⟨100⟩ direction at temperatures up to 1200° C. Elkington, Thomas, and Washburn have studied the dislocation "debris" in slip bands of MgO specimens deformed at temperatures up to 1300° C using the thin foil transmission electron microscope technique.[11] Day and Stokes have recently reported on deformation studies of MgO single crystals pulled in a ⟨100⟩ direction at a constant crosshead displacement rate at temperatures up to 2000° C.[12] Hulse, Copley, and Pask[13] have reported stress-strain curves up to 1200° C for single crystals compressed in a ⟨111⟩ direction and have shown that, above 350° C, specimens oriented in this way deform on the $\{100\}\langle 01\bar{1}\rangle$ slip systems.

In this investigation, stress-strain curves are presented for both ⟨100⟩ and ⟨111⟩ oriented single crystals, compressed at a constant stress rate at temperatures ranging from 1000 to 1600° C. The effect of varying the stress rate and the static recovery behavior have also been investigated. Stress-strain results have been analyzed by extending the dynamic approach developed by Johnston and Gilman, for explaining the yield behavior of LiF single crystals in a constant displacement rate test, to the constant stress rate method of testing used in this investigation.[2,14]

II. EXPERIMENTAL PROCEDURE

(1) MgO Single-Crystal Specimens

Specimens, with typical dimensions of 0.225 by 0.225 by 1 in., were prepared from aggregates of large MgO crystals obtained from the Norton

Co., Worcester, Massachusetts, and from the Muscle Shoals Electrochemical Corp., Tuscumbia, Alabama.* The ⟨100⟩ loading axis specimens were formed by cleaving; the ⟨111⟩ loading axis specimens were cut as described previously.[13] After final shaping by grinding with 220A sandpaper, all specimens were polished for 1 min in 85% orthophosphoric acid at 110°C to remove part of the damage. The specimens, however, probably had many dislocation sources on their surfaces. Stress-strain curves obtained under the same experimental conditions for crystals from both sources were found to be quite similar.

(2) Stress-Strain Tests

All specimens were loaded in compression at a constant stress rate of 20 psi/sec. The reported stresses were calculated from initial sample cross sections and are actual compressive stresses. Strains were determined by measuring the displacement of two small divot holes initially 0.5 in. apart centered on a side face of the specimens. All reported strains are true strains, the true strain being equal to the natural logarithm of one plus the engineering strain.

Early experiments indicated that the specimen ends tended to translate in a plane perpendicular to the loading axis. This translation was avoided by anchoring alumina buttons, which were placed as stress distributors between the ends of the specimen and the loading rams, to the loading rams. A strong bond developed at the specimen-button interfaces, even in the presence of thin sheets of platinum that were placed there as reaction barriers. Thus, constraining the buttons constrained the specimen ends as well.

---

*Spectroscopic analyses indicated for Norton Co. crystal—Fe 0.01, Mn 0.0015, Al 0.005, Cu 0.0015, Ca 0.01, and Cr 0.001%; and for Muscle Shoals Electrochemical Corp. crystal—Si 0.004, Fe 0.006, Mn < 0.0008, Al 0.005, Cu 0.001, Ca 0.12, and Cr 0.002% (values are reported as oxides of indicated elements).

A furnace, using $MoSi_2$ hairpin-shaped elements, was constructed to enable obtaining stress-strain curves at constant temperatures up to 1600° C in air. A detailed description of the overall apparatus used in this investigation is to be published separately.[15]

III. RESULTS

(1) Stress-Strain Curves for ⟨100⟩ Stress Axis

Stress-strain curves for specimens with a ⟨100⟩ stress axis at temperatures from 1000° C to 1600° C are shown in Fig. 1. This orientation results in a maximum resolved shear stress on four of the six possible slip systems belonging to the {110} ⟨1$\bar{1}$0⟩ family; the resolved shear stress vanishes on the other two slip systems as well as on the {100}⟨01$\bar{1}$⟩ family. The four consist of two pairs of orthogonal slip systems which intersect at 60 deg. Although the behavior of individual specimens agreed quite well up to 1300° C, some variation was observed for the different specimens tested at 1400° C. It was thought that this variation might be related to differences in impurity content between specimens. Thus, the stress-strain curves for 1300, 1510, and 1600° C, shown in Fig. 1, were obtained for single crystals cleaved from the same crystal block. Figure 2 shows the yield stress values, corresponding to the stress supported by the specimens at 0.1% strain, vs temperature. Only a slight decrease in yield stress occurs for this orientation in the temperature range of 1000° C to 1600° C.

Of particular interest for temperatures above 1100° C is the change in the general shape of the stress-strain curves with the appearance of a gradual yield. This transition from an abrupt yield becomes more

apparent at higher temperatures. Specimens were not normally deformed to failure at temperatures above 1100° C; they were often strained 15% without the appearance of cracks. At 1400° C one specimen was strained 30% without the appearance of a crack.

As a measure of strain-hardening rate, the slope of the first approximately linear portion of the stress-strain curve extending over an appreciable strain is plotted vs temperature in Fig. 3. At 1100° C and below it was observed that as the stress at a given strain decreased, this slope increased. Above 1100° C this slope decreased rapidly with increasing temperature. Data points at 1000° C and below in Fig. 3 are taken from the paper by Hulse and Pask.[8]

(2) Stress-Strain Curves for $\langle 111 \rangle$ Stress Axis

Stress-strain curves for specimens with a $\langle 111 \rangle$ stress axis obtained at temperatures from 1200° C to 1600° C are shown in Fig. 4. This orientation results in an equal resolved shear stress on three of the six $\{100\}$ $\langle 01\bar{1} \rangle$ slip systems, and no stress on the $\{110\}$ $\langle 1\bar{1}0 \rangle$ family, as previously discussed.[13] It is apparent that the strain hardening is considerably greater than that observed in the curves for the $\langle 100 \rangle$ oriented specimens. This result is undoubtedly due to the long range repulsive stress interactions between intersecting dislocations arising because the Burgers' vectors of the three active slip systems are at 60 deg to one another. As a consequence it was particularly difficult to constrain the sample ends from translating in planes perpendicular to the stress axis. In the 1500 and 1600° C specimens such translation resulted from slip taking place predominately on one $\{100\}$ $\langle 01\bar{1} \rangle$ slip system as was verified by examination of slip band birefringence with polarized light.

The yield stresses for ⟨111⟩ oriented specimens were considerably greater than those for the ⟨100⟩ orientations and continuously decreased up to 1600° C, as seen in Fig. 2. The ratio of the yield stresses is about 13:1 at 350° C, 4.5:1 at 600° C, and about 2.9:1 at 1600° C.

(3) Intersection of Slip Planes

Figure 5a shows a ⟨100⟩ oriented single crystal strained 14.8% at 1400° C. An interesting feature of this specimen is the vertical striations which appear on the upper part of the front face. Figure 6 shows a {100} surface cleaved parallel to the front face of the crystal. The steps appearing on this surface show that there are dislocation boundaries that go back from these striations through the volume of the crystal. Figure 7 shows a {100} surface cleaved perpendicular to the front face of the crystal and also perpendicular to its stress axis. The steps on this surface indicate that the dislocation boundaries lie on {110} planes.

These striations and dislocation boundaries are associated with deformation bands resulting from the separation of regions that have deformed by slipping on planes at 45 deg to the crystal surface (bulging bands) from those that have slipped on planes at 90 deg (flat bands). At temperatures up to 1600° C, slip in a given region of a specimen deformed in this orientation was observed to occur only on two slip planes at 90 deg to each other. Slip on one such orthogonal set of slip systems apparently blocks slip on the other orthogonal set even though both sets have the same resolved shear stress. It is thus indicated that even at the highest test temperatures the 60-deg intersections of the Burgers' vectors are considerably more difficult than the 90-deg intersections.

Figure 5b is a photograph of the same specimen under polarized light. The birefringence is a result of elastic distortion in regions where the density of dislocations of one sign is great. The localization of dislocation damage as indicated by this photograph is particularly interesting since the etched crystal surface gave little indication that such localization might exist. Etching revealed only a dense continuum of pits.

(4) Effect of Stress Rate

The effect of various stress rates on the plastic deformation of ⟨100⟩ oriented specimens at 1321°C is shown in Fig. 8. At a given strain, the slope of the stress-strain curve generally decreases with a decrease in the loading rate, as was the case at room temperature.[9] The effect on the bulk yield stress was slight, although there was a decrease with decrease in loading rate. None of the specimens showed any fractures up to the test limit of 15% strain.

(5) Recovery Experiments

Figures 9 and 10 show the results of static recovery experiments carried out at 1000 and 1400°C for specimens compressed in the ⟨100⟩ direction with a stress rate of 20 psi/sec during the loading periods. The specimens were yielded, unloaded for a period of time, and then yielded again. This cycle was repeated several times. The stress-strain curve obtained at 1000°C, following this procedure, is particularly interesting because the abrupt yielding followed by a high strain rate indicates that a pinning of dislocations, probably by diffusion of impurity atoms to them, occurred while the specimen was unloaded. This result is consistent with previous observations by Elkington et al.[6] and

also by May and Kronberg[10] of the appearance of a yield point for MgO deformed above 750° C.

Some idea of the rate of pinning can be obtained by comparing the results of unloading the specimen for various lengths of time. Little pinning was observed after unloading the specimen for 2 min, but the 5-min period produced as much pinning as the 30-min one.

At 1400° C the static recovery behavior of MgO is quite similar to that of a metal deformed at a temperature exceeding half its melting point. Much of the dislocation damage introduced during plastic straining anneals out during the unloaded periods. This "annealing-out" appears to occur quite rapidly. The term "orthorecovery" has often been used to describe this behavior in metals.

IV. DISCUSSION

(1) The Slope of the Stress-Strain Curve at Constant Stress Rate

The slope of stress-strain curves obtained at a constant stress rate is related to the plastic strain rate by the equation

$$\frac{d\sigma}{d\epsilon} = \frac{d\sigma}{dt}\left(\frac{d\epsilon}{dt}\right)^{-1} . \qquad (1)$$

The plastic strain rate can be related to dislocation behavior by the equation

$$\frac{d\epsilon}{dt} = \dot{\epsilon} = m \rho b \bar{v} , \qquad (2)$$

where ρ is the total length of mobile dislocation in the crystal divided by the crystal volume, b is the magnitude of the Burgers' vector,

$\bar{v}$ is the average dislocation velocity, and m is a geometrical constant equal to 1/2 for single crystals of MgO stressed in a ⟨100⟩ direction.

Johnston and Gilman's[2] measurements of dislocation velocities in LiF and Johnston's[3] measurements of dislocation velocities in MgO show that the velocity of screw and edge dislocations is related to the resolved shear stress by an equation of the form

$$v = v_o \left(\frac{T}{T_o}\right)^n , \tag{3}$$

where T is the resolved shear stress, v_o equals 1 cm/sec, and T_o and n are constants. Johnston and Gilman also found that in LiF edge dislocations travel at a substantially greater velocity than screw dislocations. Because of this velocity difference they show that

$$\bar{v} \cong 2\, v_s , \tag{4}$$

where v_s is the velocity of screw dislocations.

Equations (1) to (4) can be combined to give

$$\frac{d\sigma}{d\epsilon} = \frac{1}{\rho\, b\, v_o\, (T/T_o)^n} \frac{d\sigma}{dt} , \tag{5}$$

where m has been set equal to 1/2 and T_o is the appropriate constant for screw dislocations. Thus, if (a) the constants T_o and n, (b) the shear stress acting on mobile dislocation line, and (c) the variation of ρ during plastic deformation are known, the slope of the stress-strain curve at constant stress rate can be predicted.

(2) Yielding Dynamics at Room Temperature

During the bulk yielding of MgO single crystals at room temperature, both the shear stress acting on a mobile dislocation line and the

variation of ρ during plastic deformation are known. The shear stress acting on a dislocation moving through undeformed crystal is just the resolved shear stress calculated from the applied load. Also, because dislocation movement is restricted to slip band edges, ρ is proportional to the amount of interface area between slip bands and undeformed crystal.[7] Thus, for specimens in which a moderate number of slip bands form, ρ should change rapidly during the period of slip band formation early in yielding when the strain rate is small and then remain essentially constant during yielding. If T in equation (5) is set equal to the resolved shear stress, $\frac{1}{2}\sigma$, and ρ is held constant, equation (5) may be integrated to give directly the stress-strain curve at small strains,

$$\epsilon = \frac{v_o b}{n+1} \left(\rho\, \sigma_o^{-n}\right) \left(\frac{d\sigma}{dt}\right)^{-1} \sigma^{n+1} , \qquad (6)$$

where $\sigma_o = 2\, T_o$. If $\rho\, \sigma_o^{-n}$ and n were known for the crystals used in this investigation, a direct comparison could be made between theoretical and experimental stress-strain curves. Because these parameters are not known, the consistency of equation (6) with experimental stress-strain curves was checked by determining whether it could reproduce such curves based on reasonable values for $\rho\, \sigma_o^{-n}$ and n.

Curve A in Fig. 11 was thus calculated from equation (6), with $\rho\, \sigma_o^{-n}$ and n chosen so that curve A would match curve B which is the 26° C curve shown in Fig. 1. The best match was obtained by setting n equal to 33 and $\rho\, \sigma_o^{-33}$ equal to 4.82×10^{-135} cm^{-2} psi^{-33}. This value of n is similar to values obtained by direct measurement of dislocation velocities in LiF and MgO.[2,3] It will be shown that the value given for

$\rho\ \sigma_o^{-n}$ is also quite reasonable (a) by establishing an upper limit for σ_o (assuming that n equals 33), and (b) by showing that the corresponding upper limit for ρ, as determined by the condition that $\rho\ \sigma_o^{-n}$ be equal to 4.82×10^{-135} cm^{-2} psi^{-33} is consistent with the results of etch pit studies.

The distance, d, that a dislocation moves during a time t can be obtained by integrating equation (3) (T and T_o have been replaced by σ and σ_o)

$$d = v_o \int_o^t \left(\frac{\sigma\ (t)}{\sigma_o} \right)^n dt\ . \qquad (7)$$

An upper limit for σ_o can, therefore, be calculated based on the fact that screw dislocation bands were observed in the gage sections of specimens deformed at room temperature at about 0.1% strain. In the case of the specimen whose stress-strain behavior is represented by curve B, a strain of 0.1% corresponded to a compressive stress of about 14,800 psi. The stress rate for this specimen was 20 psi/sec and thus, at this stress, loading had been in progress for 740 sec. The formation of screw dislocation bands could not have occurred unless screw dislocations had moved at least 3 mm. Thus, an upper limit can be set for T_o by making the appropriate substitutions in equation (7) and by carrying out the integration. The calculated upper limits for σ_o and ρ are given in Table I.

Washburn and Gorum[6] have estimated the number of etch pits formed in an edge dislocation band of MgO to be on the order of 10^9 cm^{-2}. Edge dislocation bands were about 1 cm long in the compression specimens, and the total number of dislocation bands formed in the gage sections of

specimens with a moderate amount of surface damage was about 200. If it is assumed that 1/50 of the etch pits lying within 0.1μ of slip band edges corresponded to mobile dislocations, on the basis that (a) only dislocations lying close to slip band edges can be mobile, and (b) most of the etch pits in edge dislocation bands correspond to dislocation dipoles; then, ρ should be about $2(200) \times 10^{-5} \times 1 \times 10^{9} \times \frac{1}{50} = 8 \times 10^{4}\ cm^{-2}$. This value is in reasonable agreement with the calculated upper limit and thus it is concluded that both the values for n and $\rho\ \sigma_o^{-n}$ used to "fit" curve B are consistent with the known experimental facts.

It is of particular interest that additional assumptions with regard to unpinning of dislocations or the sudden generation of mobile dislocation line by dipoles are not necessary to explain the shape of the stress-strain curve at room temperature. The curve is determined by the stress dependence of the dislocation velocity. The agreement of the calculated and experimental curves supports that slip band formation in the specimen occurred at strains less than 0.001.

(3) Yielding Dynamics at Elevated Temperatures

No measurements have yet been reported of the temperature variation of average dislocation velocities in MgO. Such measurements have been made, however, for LiF over a relatively narrow temperature range which showed that increasing the temperature from 77 to 300°K decreased T_o while n remained about constant.[2] Assuming a similar behavior in MgO, curve C in Fig. 11 was calculated with the same values of ρ and n as curve A but with σ_o adjusted to give the same yield stress as curve D which is the 1000°C in Fig. 1. This curve and the experimental curve D

both show a sharp yield as predicted by equation (6). The increased slope of the experimental curve beyond the yield is due to strain hardening which occurs at small strains. This behavior suggests that dislocation interactions exist at small strains at 1000° C which do not occur at room temperature and which are not taken into account by the equation.

On the basis of the dominant role of dislocation mobility in determining the shape of the stress-strain curve at room temperature and the temperature dependence of dislocation mobility observed in the case of LiF, the most straightforward explanation for the decrease in yield stress for ⟨100⟩ stressed specimens with increasing temperature would appear to be increased dislocation mobility. A difference in dislocation mobility is also probably responsible for the difference in yield stress between specimens stressed in ⟨100⟩ and ⟨111⟩ directions. When a dislocation moves on a {110} plane, ions of opposite sign approach each other at the core of the dislocation in a "midglide" position. For dislocation movement on {100} planes, on the other hand, Gilman has pointed out that strong repulsive forces develop because ions of like sign are forced to approach each other.[16] Because of this structural reason for the difference in dislocation mobility on {100} and {110} planes, it seems unlikely that the bulk yield stress of ionic single crystals with the NaCl structure should be the same for both slip systems at temperatures up to the melting point.

Curve E in Fig. 11 is a curve calculated using equation (6) with σ_o, ρ, and n chosen to match curve F which is the 1300° C curve from Fig. 1. In this case, the best match was obtained by choosing n to be about 2. Thus, at 1300° C the strain rate is much less sensitive to stress

than at 1000° C. Similar shapes were observed for all specimens tested above 1100° C. It is likely that this decrease in stress sensitivity is due to a decrease in the stress sensitivity of the dislocation velocity. Such a decrease might occur, for example, if dislocation motion becomes limited by the nonconservative motion of jogs. It is doubtful, however, that the assumptions made in developing equation (6) are valid above 1100° C.

Equation (6), for example, does not correctly predict the effect of varying the stress rate at 1300° C as it does at room temperature. This condition becomes apparent by comparing the experimental curves in Fig. 8 with curves G-80, G-2, and G-20 (same as E) in Fig. 11 which were calculated using the same values of ρ, σ_o, and n as curve E. Although the calculated curves predict qualitatively the correct behavior, the agreement with respect to the magnitude of the stress rate effect is poor. It thus appears that one or more of the assumptions used to derive equation (6) no longer apply: the dislocation velocity may no longer be represented by equation (3); the shear stress acting on moving dislocations may no longer be that calculated from the applied load due to interactions between dislocations arising from a change in the distribution of dislocations at small strains; or the parameter ρ may no longer be constant in the yield region. The implied decrease in the stress dependence of the dislocation velocity would also cause ρ to play a greater part in determining the shape of the stress-strain curve during yielding.

(4) Strain Hardening

A material is said to strain harden if its yield stress increases upon reloading after an increment of plastic strain; the slope of a

stress-strain curve is thus often taken as a measure of strain-hardening rate. In making such an interpretation, however, it must be realized that the resistance of a test specimen to dislocation motion may vary considerably from region to region because of inhomogeneity of dislocation damage and that the slope of the stress-strain curve at a given strain indicates only the resistance to dislocation motion in the region where such resistance is least.

For a given applied load, strain hardening results from a decrease of the net shear stress acting on moving dislocations due to stress interactions between the moving dislocations and other dislocations and defects present in the deformed volume. It can also occur in a compression specimen as a result of lattice rotation relative to the compression axis. A decrease of the net shear stress acting on moving dislocations causes them to move more slowly or to stop moving altogether. Thus, the length of moving dislocation line, the average dislocation velocity, and consequently the strain rate all decrease for a given applied load.

Figure 3 shows that $\frac{d\sigma}{d\epsilon}$ measured at the first approximately linear part of the stress-strain curve is about twice as large at 1000° C as it is at 26° C. The reason for this increase is not clear. Information on the distribution of dislocations in deformed crystals at various stages of deformation as a function of temperature is needed to properly interpret this effect. Etch pit and stress birefringence techniques are now being used to obtain such information.

Beyond 1100° C, $\frac{d\sigma}{d\epsilon}$ begins to decrease rapidly with increasing temperature and by 1600° C has decreased by a factor of about 8. It seems likely that this decrease results from the rapid "annealing-out" of

dislocation dipoles due to increased diffusion rates in this temperature range. Washburn et al.[5] and also Elkington et al.[11] have observed that dislocation dipoles in MgO are not stable at elevated temperatures and pinch off into a series of small prismatic loops separated by distances of several times their diameter. The annealing-out of this type of defect probably accounts for much of the recovery observed in the static recovery experiment at 1400° C.

The static recovery experiment at 1400° C also indicates that a part of the dislocation damage produced at 1400° C is stable and interferes with further dislocation movement. At each successive loading, yielding occurred at a higher stress. The results of the stress rate experiments shown in Fig. 8 also indicate that thermally stable dislocation damage is produced which accumulates with increasing strain. This effect can be seen by comparing the strain rates at 10,000 psi for the various constant stress rate curves (Table II). The smallest strain rate was observed at 2 psi/sec because this specimen had strained the most even though the time to anneal out thermally unstable damage was greatest for this stress rate.

One type of dislocation damage stable at 1400° C is that represented by the dislocation boundaries associated with the vertical striations on the surface of the specimen shown in Fig. 5a. As pointed out earlier, these boundaries separate regions that have deformed on slip planes at 90 deg and 45 deg to the specimen surface.

Two types of dislocation boundary can be formed by dislocations moving on oblique {110} planes, as discussed by Kear, Taylor, and Pratt.[17]

a) Dislocations moving on oblique planes with Burgers' vectors that enclose an angle of 60 deg experience a repulsive force. Reactions of the type

$$\frac{a}{2}[\bar{1}01] + \frac{a}{2}[0\bar{1}1] = \frac{a}{2}[\bar{1}\bar{1}2] \qquad \text{(i)}$$

do not occur because they cause an increase in elastic energy. A boundary may form, however, which can lie on any contact plane.

b) Dislocations moving on oblique planes with Burgers' vectors that enclose an angle of 120 deg experience an attractive force. A reaction of the type

$$\frac{a}{2}[\bar{1}01] + \frac{a}{2}[01\bar{1}] = \frac{a}{2}[\bar{1}10] \qquad \text{(ii)}$$

can occur to form segments of edge dislocation line lying along the $[11\bar{1}]$ direction. These segments can move only in the $(11\bar{2})$ planes and are therefore sessile. A boundary can form which in the case of (101) $\frac{a}{2}[\bar{1}01]$ and (011) $\frac{a}{2}[0\bar{1}1]$ dislocations lies on the $(1\bar{1}0)$ plane and consists of $\frac{a}{2}[\bar{1}10]$ edge dislocations lying one above the other and parallel to $[11\bar{1}]$.

Each of the boundaries described above has a [111] rotation axis as determined by the cross product $b_1 \times b_2$. Thus, the first boundary with a (110) contact plane is a mixed tilt-twist boundary, while the second with a contact plane of $(1\bar{1}0)$ is a pure tilt boundary. The mixed type of boundary has been reported to form in squat compression specimens of NaCl and KCl by Taylor and Pratt.[18] Such boundaries are high energy boundaries, however, and should be rather diffuse; it thus seems unlikely that they are responsible for the stable, sharp boundaries lying on {110} planes that were observed in our specimens. These boundaries are thought to be the pure tilt boundaries. They have previously been observed to form

in NaCl, LiF, and MgO bend specimens by Stokes, Johnston, and Li.[19] Boundaries of this type will remain sessile unless some complex dislocation movement takes place such as glide on {112} planes, thus explaining their persistence up to 1600° C. They attract or repel dislocations with a force which decreases gradually with temperature because their only temperature dependence comes from the decrease in the shear modulus.

V. SUMMARY

Stress-strain curves have been obtained for single crystals of MgO deformed at constant stress rate in compression at 26° C and at 1000 to 1600° C in ⟨100⟩ and ⟨111⟩ orientations. Below 1200° C, the experimental curves are consistent with the hypothesis that yielding behavior is determined primarily by the dislocation mobility due to a large n in equation (3). Above 1100° C, the strain rate becomes much less stress sensitive. This fact suggests that the dislocation velocity may be less stress sensitive and that ρ, the length of dislocation line, therefore, plays a greater part in determining yield behavior (n is small).

Also, above 1100° C the strain-hardening rate was observed to decrease and cleavage fracture was no longer observed in specimens deformed up to 15% at these loading rates. At 1400° C, "orthorecovery" was observed which was not the case at 1000° C. All these effects are believed to be related to the onset of rapid diffusion. The "annealing-out" of dipoles greatly decreases the dislocation density and, thus, the resistance encountered by dislocations as they move through the crystal. There exists between dislocations moving on oblique slip planes, however, a long range stress interaction because their Burgers' vectors enclose an

angle of 60 deg (or 120 deg). These dislocations can react to form sessile boundaries which interfere with dislocation movement. Such boundaries cannot disperse until some complex dislocation movement takes place such as glide on {112} planes.

The resistance to dislocation motion on {100} planes in the ⟨111⟩ specimens is high because in this orientation the Burgers' vectors of the three active slip systems are at 60 deg (or 120 deg) to each other. It would also be predicted on the basis of structural considerations that the mobility of dislocations on {100} planes would always be less than on {110} planes. The yield stress, however, for ⟨111⟩ oriented crystals continuously approached the yield stress for crystals with a ⟨100⟩ stress axis from 1000 to 1600°C. On the basis of experiments with LiF, it would be expected that a sharp change in slope of the yield stress vs temperature curve would occur at some temperature slightly above 1600°C.[20]

ACKNOWLEDGMENTS

The authors would like to express their thanks to N. E. Olson and M. Mendelson who assisted with the experimental phase of this investigation, and to Professor Jack Washburn for many helpful discussions.

This work was done under the auspices of the U. S. Atomic Energy Commission.

REFERENCES

1. R. J. Stokes, T. L. Johnston, and C. H. Li, "Effect of Surface Condition on the Initiation of Plastic Flow in Magnesium Oxide," Trans. AIME, 215, 437-44 (1959).
2. W. G. Johnston and J. J. Gilman, "Dislocation Velocities, Dislocation Densities, and Plastic Flow in LiF Crystals," J. Appl. Phys., 30 [2], 129-44 (1959).
3. W. G. Johnston (Research Laboratory, General Electric Company, Schenectady, New York), unpublished data.
4. J. Washburn, A. Kelly, and G. K. Williamson, "Direct Observation of Dislocations in Magnesium Oxide," Phil. Mag., [8], 5 [58], 192-93 (1960).
5. J. Washburn, G. W. Groves, A. Kelly, and G. K. Williamson, "Electron-Microscope Observations of Deformed Magnesium Oxide," Phil. Mag., [8], 5 [58], 991-99 (1960).
6. J. Washburn and A. E. Gorum, "Growth of Slip Bands and Nucleation of Cracks in Magnesium Oxide," Mem. Sci. Rev. Met., 57 [1], 67-72 (1960).
7. D. B. Hoover and J. Washburn, "Tensile Behavior of Lithium Fluoride," J. Appl. Phys., 33 [1], 11-14 (1962).
8. C. O. Hulse and J. A. Pask, "Mechanical Properties of Magnesia Single Crystals in Compression," J. Am. Ceram. Soc., 43 [7], 373-78 (1960).
9. D. S. Thompson and J. P. Roberts, "Flow of Magnesium Oxide Single Crystals," J. Appl. Phys., 31 [2], 433-34 (1960).
10. J. E. May and M. L. Kronberg, "Temperature Dependence of Plastic Yield Stress of Single Crystals of Magnesium Oxide," J. Am. Ceram. Soc., 43 [10], 525-30 (1960).

11. W. E. Elkington, G. Thomas, and J. Washburn, "Damage Produced by Moving Dislocations in MgO," J. Am. Ceram. Soc., 46 [7], 307-13 (1963).

12. R. B. Day and R. J. Stokes, "The Mechanical Behavior of Magnesium Oxide at High Temperatures," Honeywell Research Center Report HR-64-253 (1964).

13. C. O. Hulse, S. M. Copley, and J. A. Pask, "Effect of Crystal Orientation on Plastic Deformation of Magnesium Oxide," J. Am. Ceram. Soc., 46 [7], 317-23 (1963).

14. W. G. Johnston, "Yield Points and Delay Times in Single Crystals," J. Appl. Phys., 33 [9], 2716-30 (1962).

15. C. O. Hulse and S. M. Copley, "High-Temperature Compressive Deformation Equipment," to be submitted to J. Am. Ceram. Soc.

16. J. J. Gilman, "Plastic Anisotropy of LiF and Other Rock-Salt-Type Crystals," Acta Met., 7 [9], 608-13 (1959).

17. B. H. Kear, A. Taylor, and P. L. Pratt, "Some Dislocation Interactions in Simple Ionic Crystals," Phil. Mag., [8], 4 [58], 665-72 (1959).

18. A. Taylor and P. L. Pratt, "The Transient Conductivity Increase in Deformed Alkali Halides," Phil. Mag., [8], 3 [33], 1051-52 (1958).

19. R. J. Stokes, T. L. Johnston, and C. H. Li, "Kinking and the Fracture of Ionic Solids," J. Appl. Phys., 33 [1], 62-67 (1962).

20. D. W. Budworth and J. A. Pask, "Flow Stresses on the {100} and {110} Planes in LiF, and the Plasticity of Polycrystals," J. Am. Ceram. Soc., 46 [11], 560-61 (1963).

Table I. Parameters used to calculate theoretical stress-strain curves

Curve	T °C	$\dot{\sigma}$ (psi/sec)	n	σ_o (psi)	ρ (cm/cm^3)
A	26	20	33	16,640	9.47×10^4
B	26	20	-	-	-
C	1000	20	33	4,580	9.47×10^4
D	1000	20	-	-	-
E	1321	20	2.08	142,200	9.47×10^4
F	1321	20	-	-	-
G	1321	80	2.08	142,200	9.47×10^4
	1321	20	"	"	"
	1321	2	"	"	"

Table II. Strain rates at a stress level of 10,000 psi

$\frac{d\sigma}{dt}$ (psi/sec)	$\frac{d\sigma}{d\epsilon}$ (psi)	$\frac{d\epsilon}{dt}$ (sec^{-1})	ϵ
165	1.8×10^5	0.9×10^{-3}	0.032
80	8.0×10^4	1.0×10^{-3}	0.038
20	5.0×10^4	4.4×10^{-4}	0.060
2	2.0×10^4	1.0×10^{-4}	0.080

FIGURE LEGENDS

Fig. 1. Stress-strain curves for MgO single crystals compressed with a ⟨100⟩ stress axis at various temperatures. All specimens were loaded at 20 psi/sec. The specimens deformed at 1300, 1510, and 1600° C were cleaved from the same crystal block.

Fig. 2. The yield stress vs temperature curve for crystals with ⟨100⟩ and ⟨111⟩ stress axes compressed at 20 psi/sec. The ⟨111⟩ orientation yield stress at 560° C is 71,000 psi and at 360° C is 143,400 psi.

Fig. 3. Slope of the first linear portion of the stress-strain curve vs temperature for ⟨100⟩ oriented single crystals.

Fig. 4. Stress-strain curves for MgO single crystals compressed with a ⟨111⟩ stress axis at various temperatures. All specimens were loaded at 20 psi/sec.

Fig. 5. Specimen deformed 14.8% at 1400° C

(a) illuminated by reflected light

(b) between crossed polaroids, illuminated by transmitted light.

Fig. 6. Cleaved surface parallel to the front face showing the deformation bands pictured in Fig. 5.

Fig. 7. Cleaved surface perpendicular to the front face and to the stress axis showing deformation bands.

Fig. 8. Stress-strain curves for MgO single crystals compressed with a ⟨100⟩ stress axis at various constant stress rates. The specimens deformed at 165, 80, and 20 psi/sec were all cleaved from the same crystal block.

Fig. 9. Static recovery experiment on MgO single crystal at 1000° C. Specimen loaded at 20 psi/sec.

Fig. 10. Static recovery experiment on MgO single crystal at 1400° C. Specimen loaded at 20 psi/sec.

Fig. 11. Calculated and experimental stress-strain curves for MgO single crystals deformed under various conditions. The identification of the curves is given in the text.

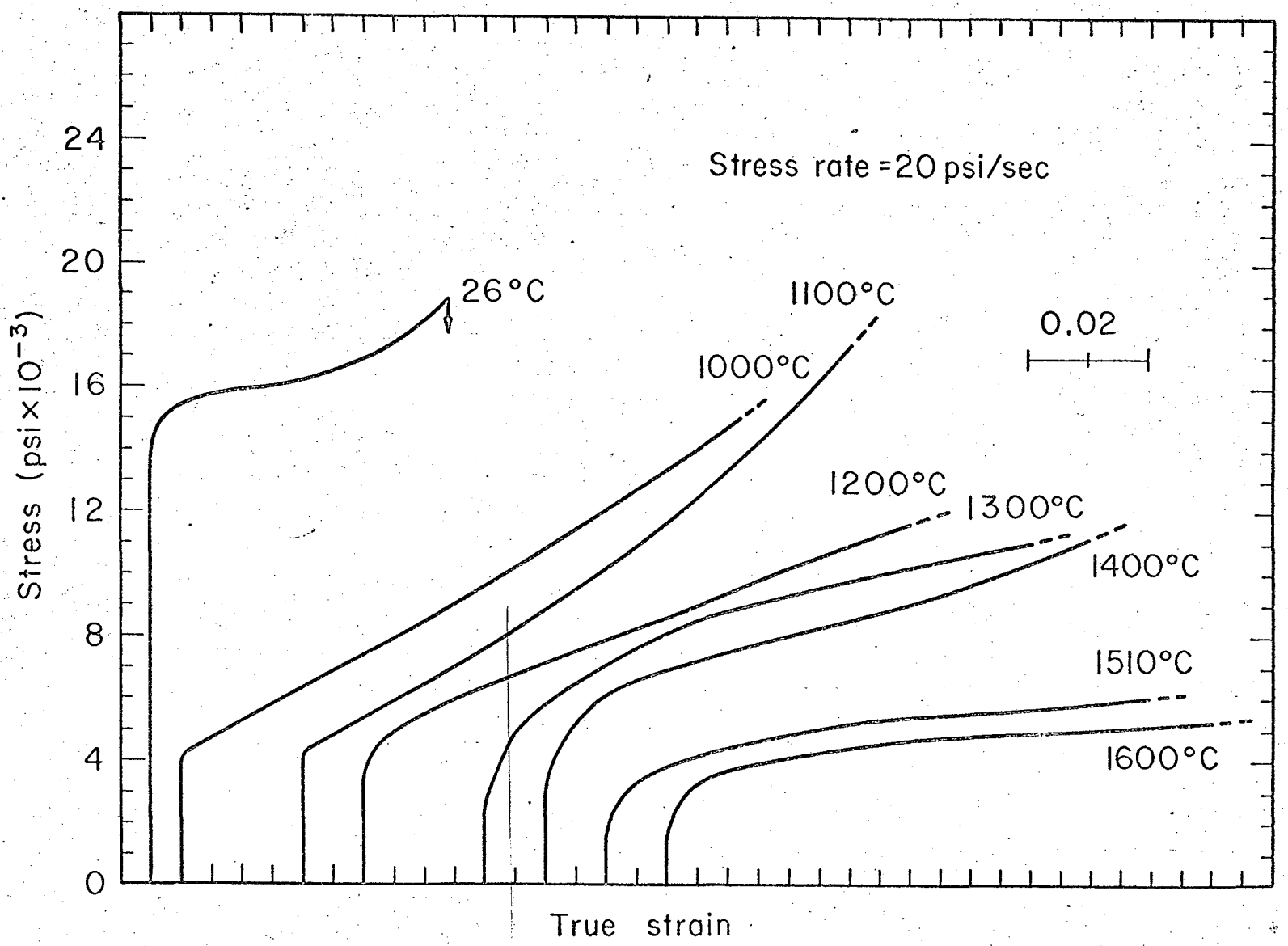

Fig. 1

MU-33614

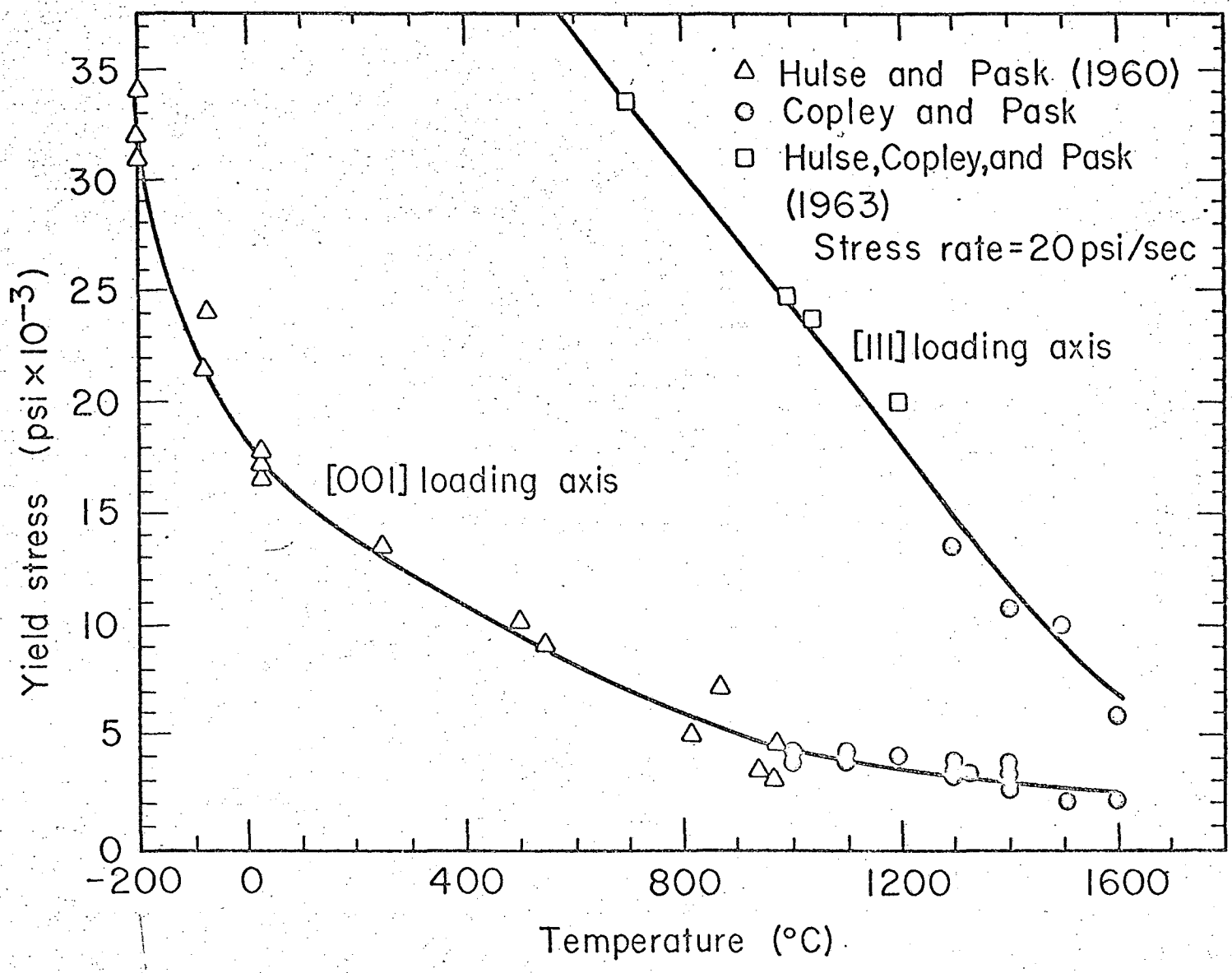

Fig. 2

MU-32270

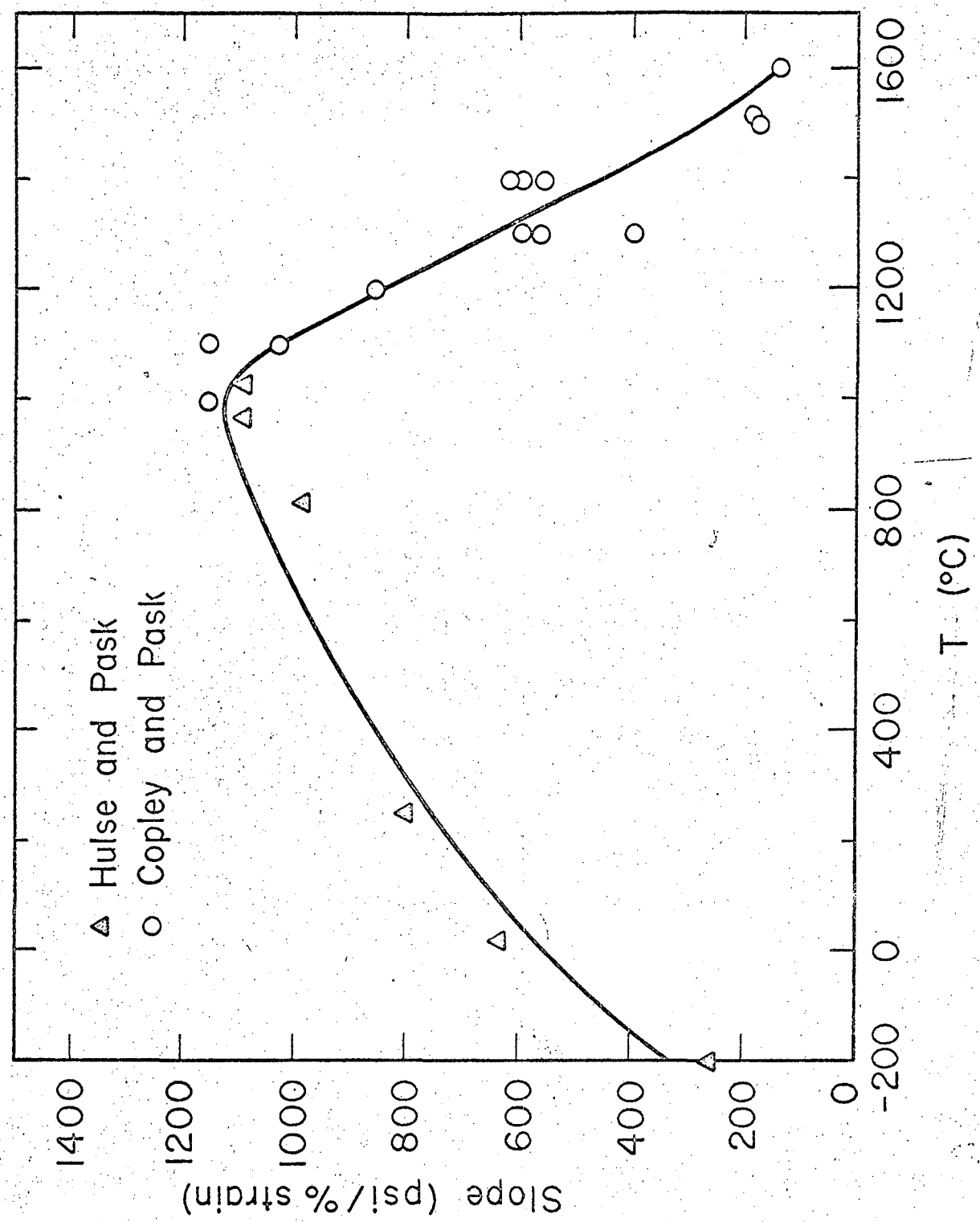

MU-32271

Fig. 3

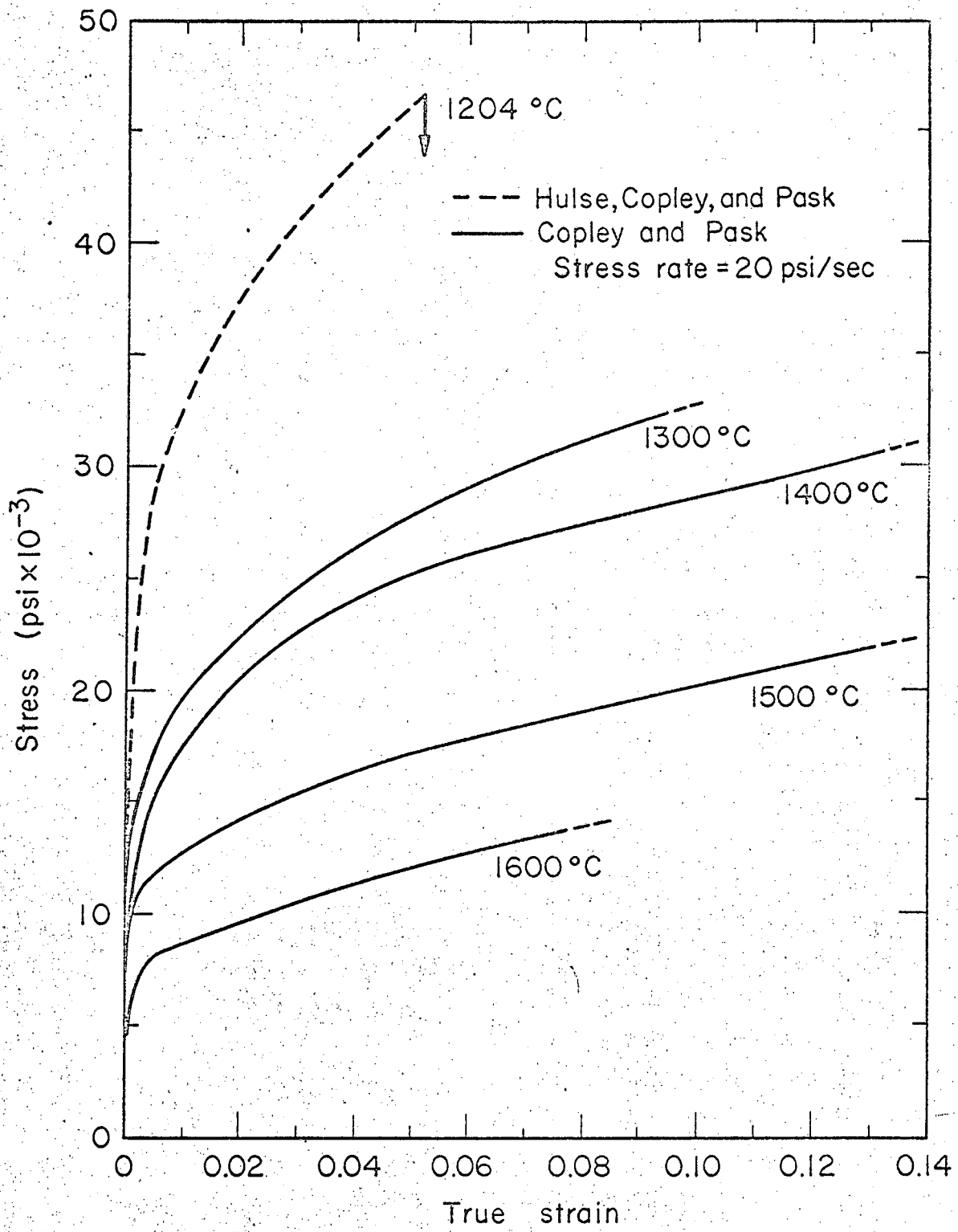

MU-32276

Fig. 4

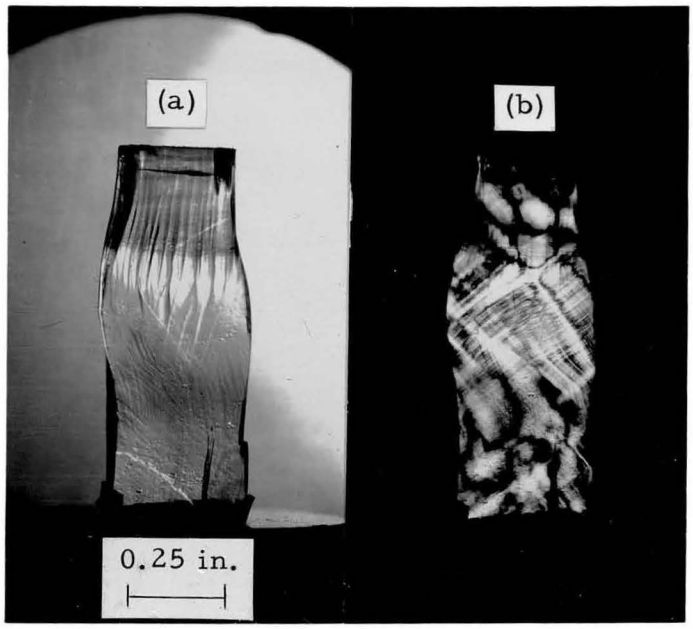

Fig. 5

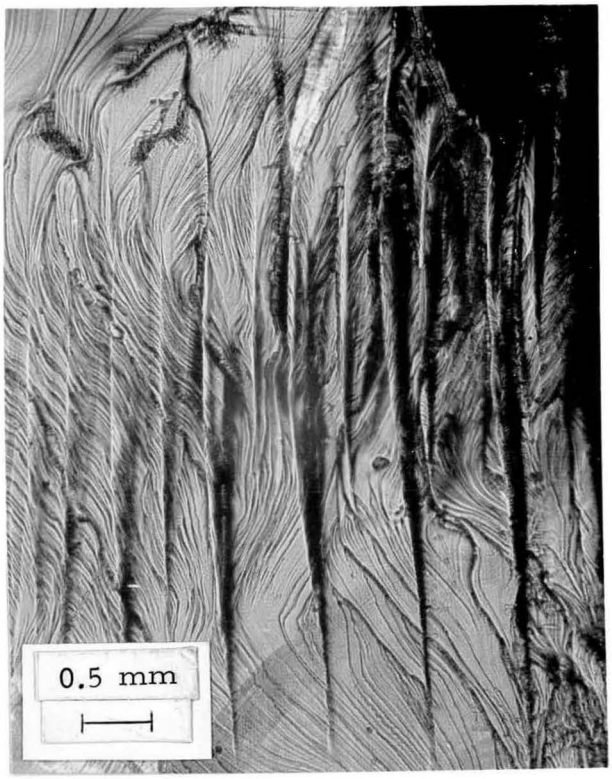

Fig. 6

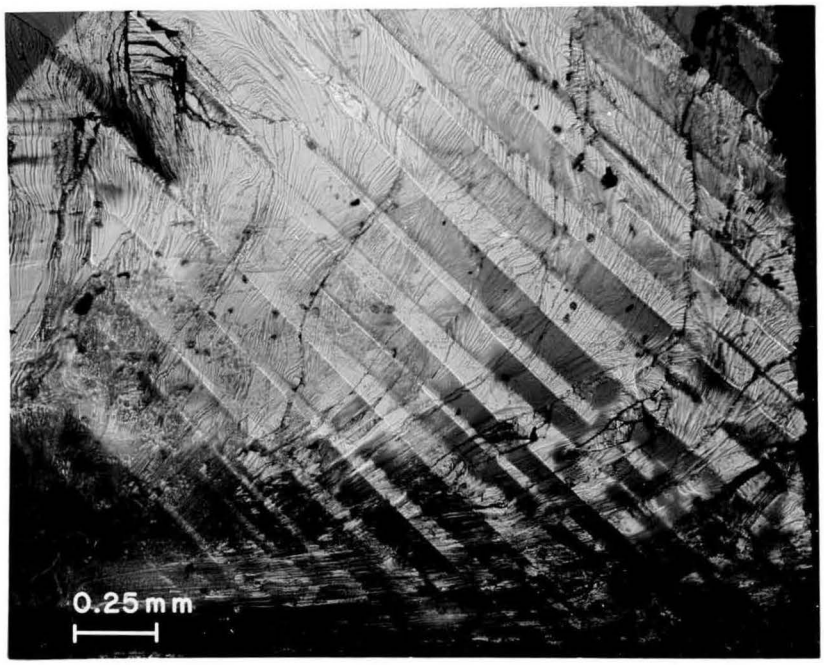

Fig. 7

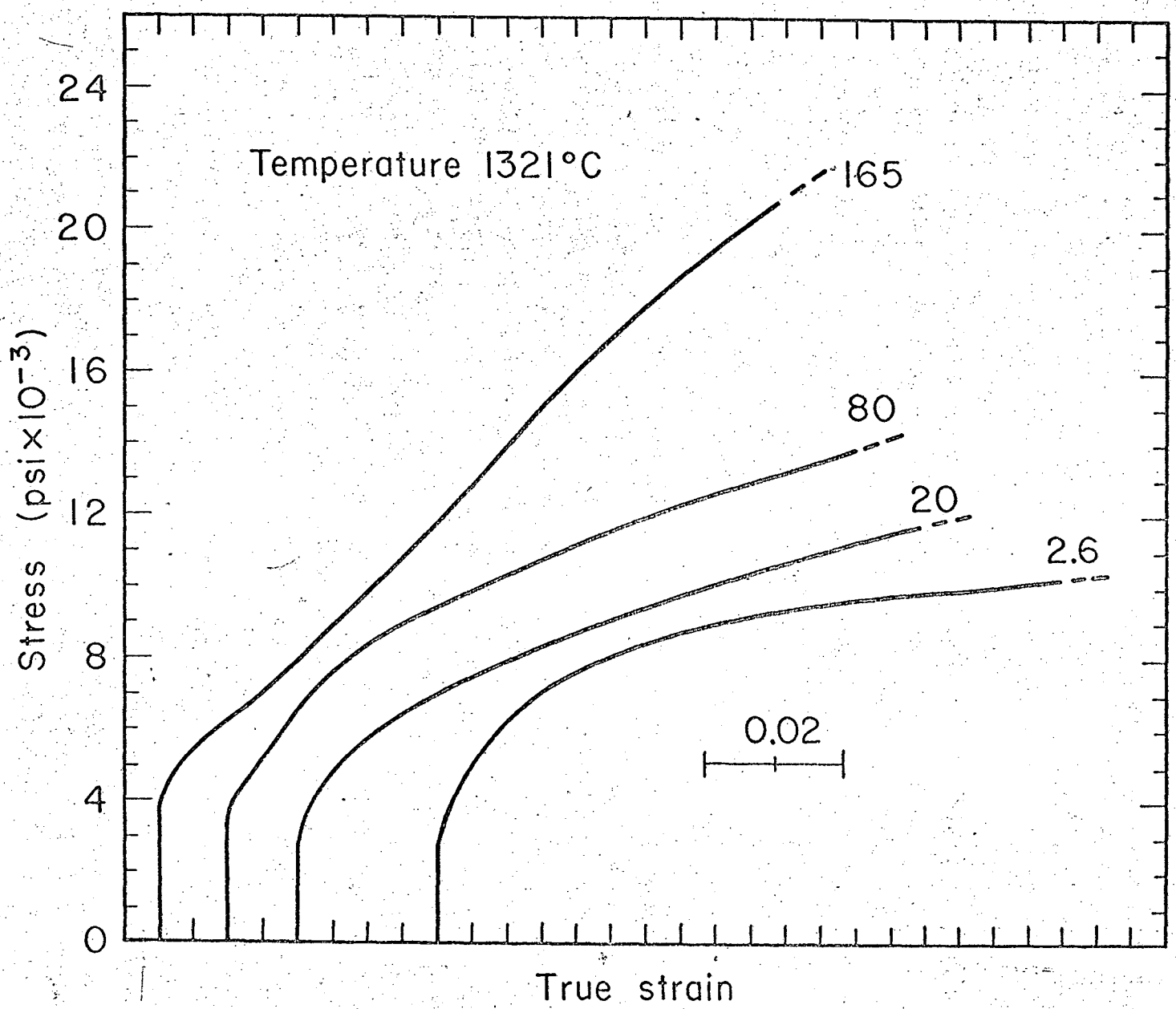

Fig. 8

MU-33615

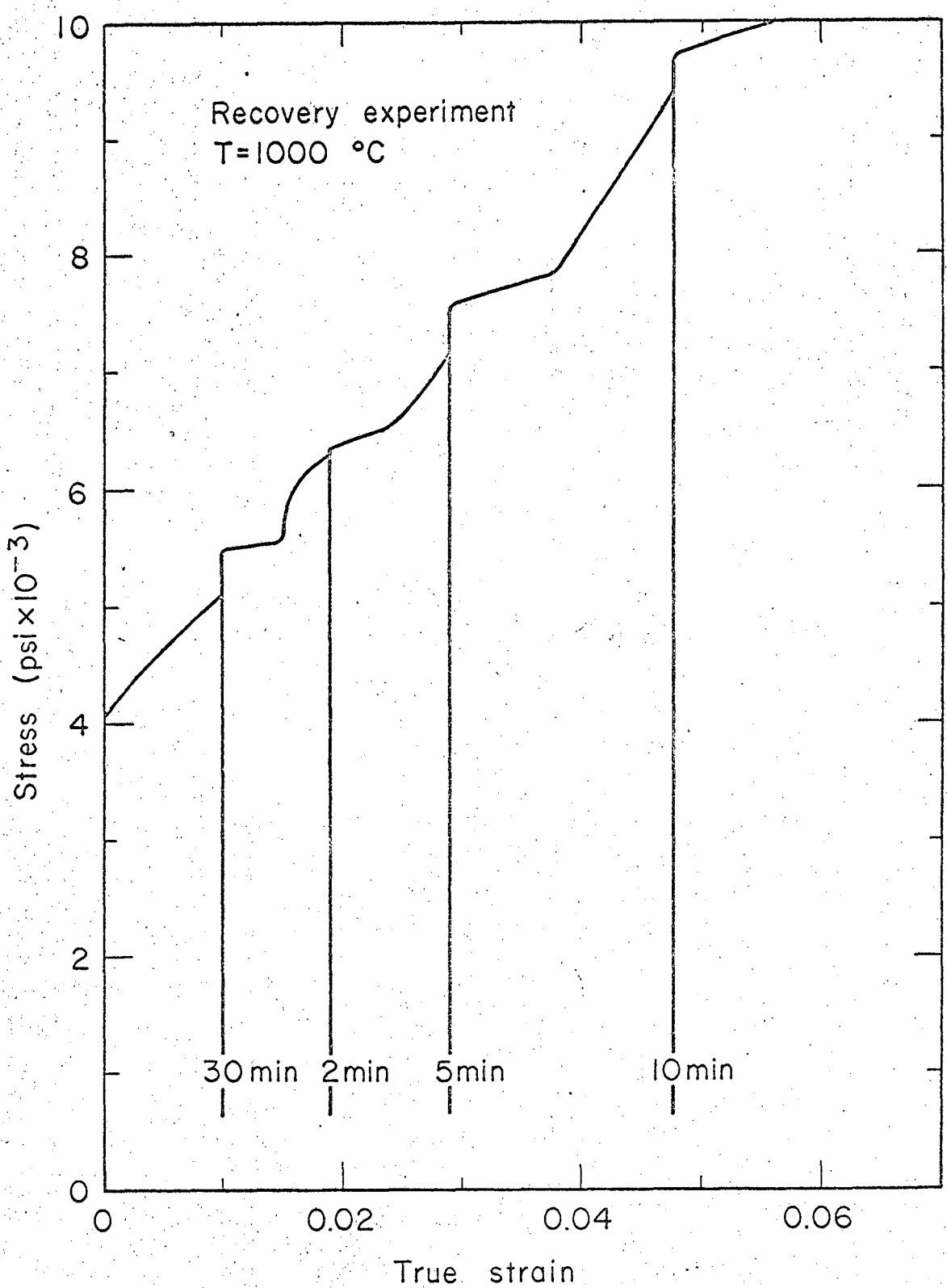

MU-32275

Fig. 9

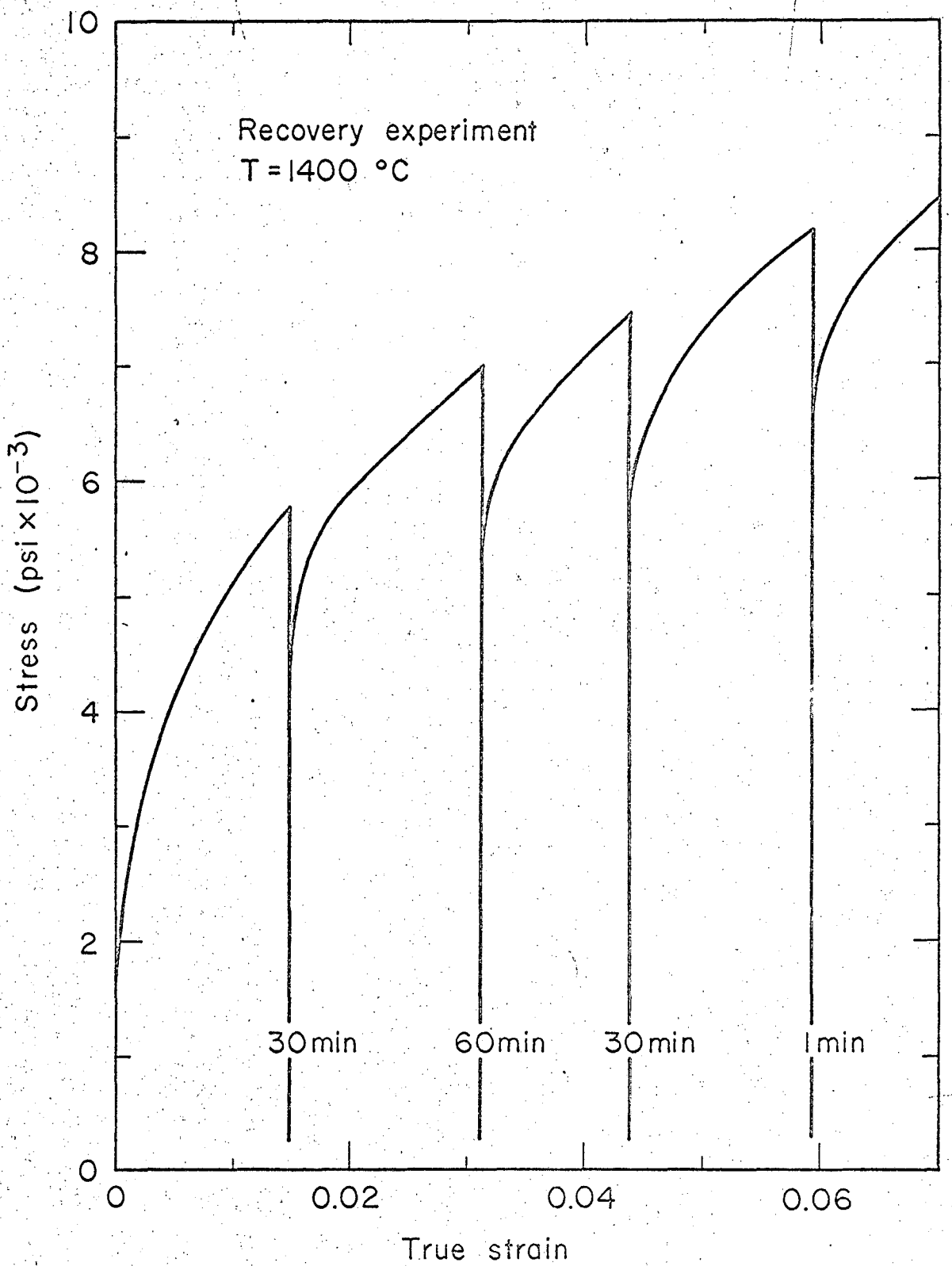

MU-32274

Fig. 10

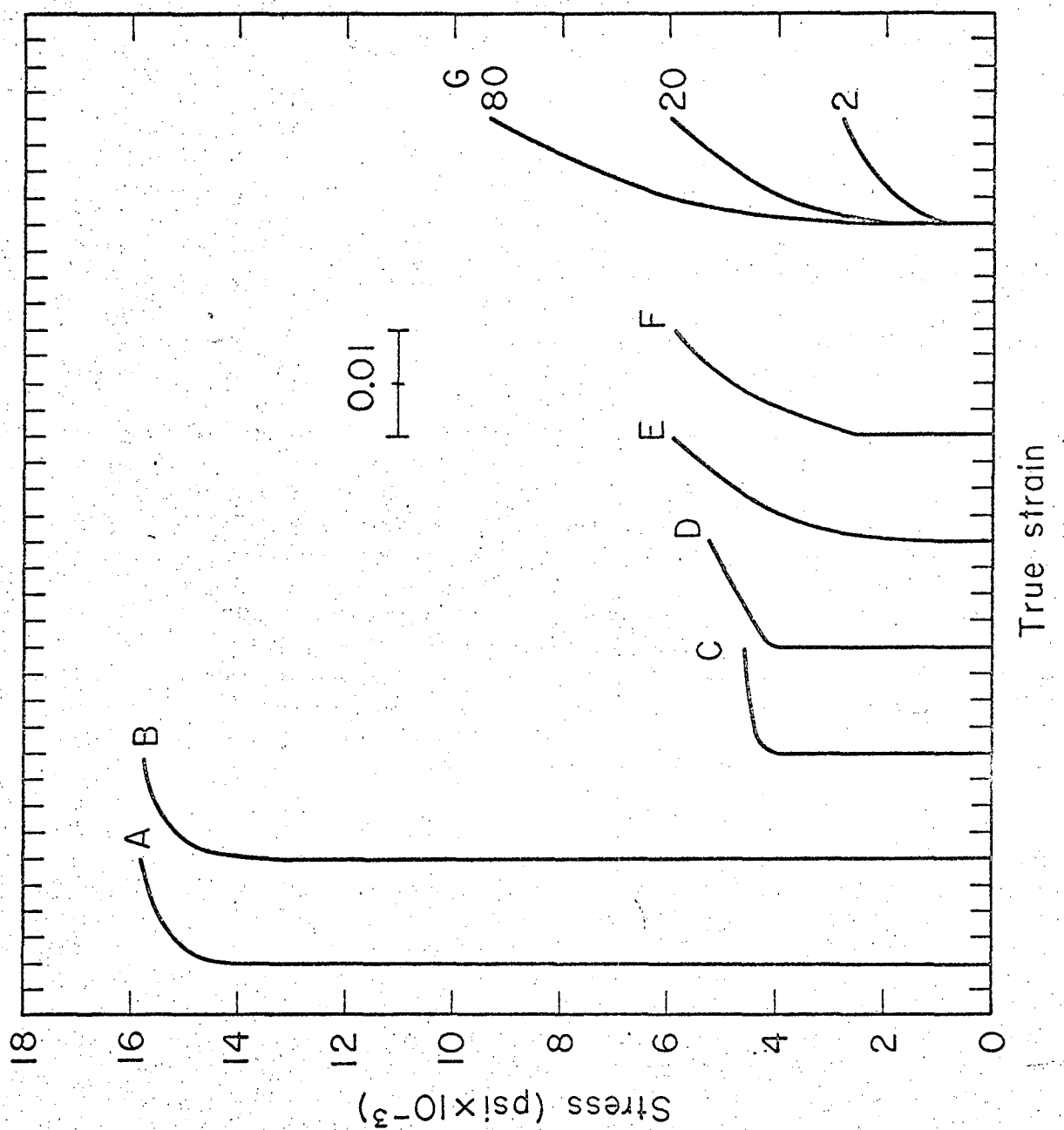

MU-33616

Fig. 11

This report was prepared as an account of Government sponsored work. Neither the United States, nor the Commission, nor any person acting on behalf of the Commission:

A. Makes any warranty or representation, expressed or implied, with respect to the accuracy, completeness, or usefulness of the information contained in this report, or that the use of any information, apparatus, method, or process disclosed in this report may not infringe privately owned rights; or

B. Assumes any liabilities with respect to the use of, or for damages resulting from the use of any information, apparatus, method, or process disclosed in this report.
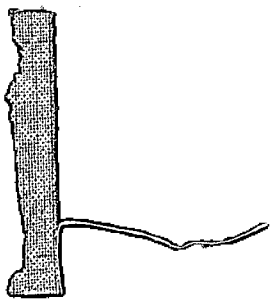
As used in the above, "person acting on behalf of the Commission" includes any employee or contractor of the Commission, or employee of such contractor, to the extent that such employee or contractor of the Commission, or employee of such contractor prepares, disseminates, or provides access to, any information pursuant to his employment or contract with the Commission, or his employment with such contractor.